Supporting information

A reversed strategy for designing high-performance anode material from traditional $Na_xV_2O_5$ cathode

Jing Yao, Meichun He, Pengju Li*, Chao Zhu, Dongmei Zhang, Cunyuan Pei, Bing Sun, Shibing Ni*

College of Materials and Chemical Engineering, China Three Gorges University, Yichang, 443002, PR China

* Corresponding author (email: lipengju11@126.com (P. Li); shibingni07@126.com (S. Ni))

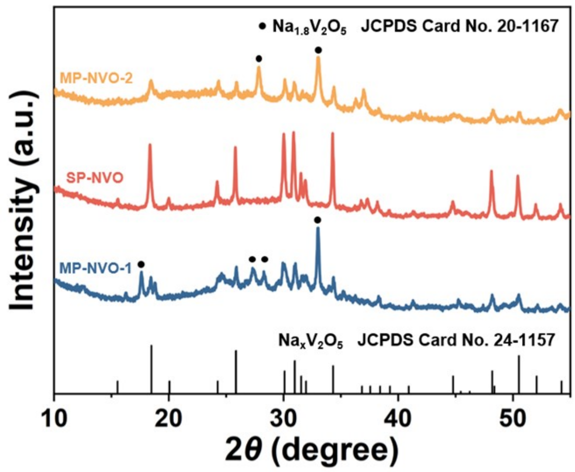

Fig. S1 XRD patterns of MP-NVO-1, SP-NVO and MP-NVO-2.

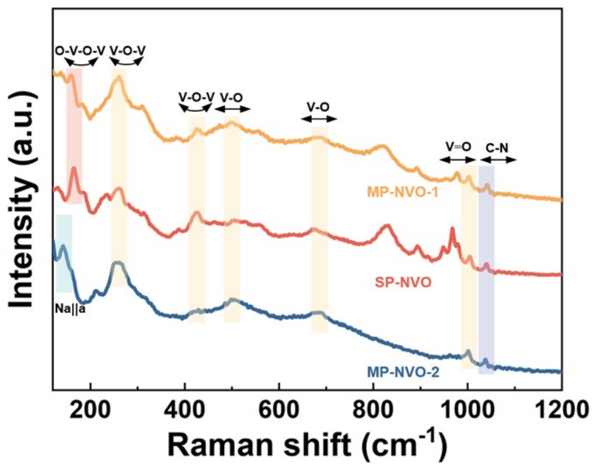

Fig. S2 Raman spectra of MP-NVO-1, SP-NVO and MP-NVO-2.

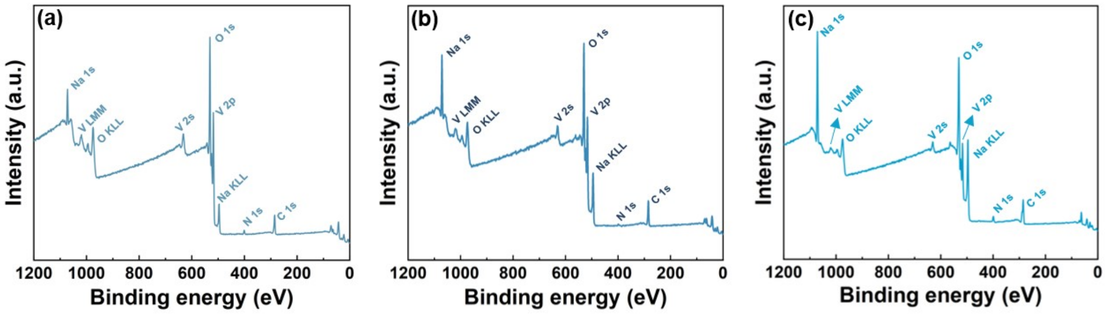

Fig. S3 XPS surveys of (a) MP-NVO-1, (b) SP-NVO and (c) MP-NVO-2.

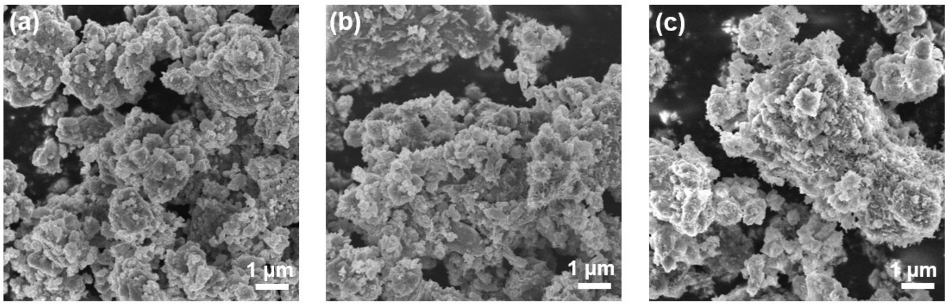

Fig. S4 SEM images of (a) MP-NVO-1, (b) SP-NVO and (c) MP-NVO-2.

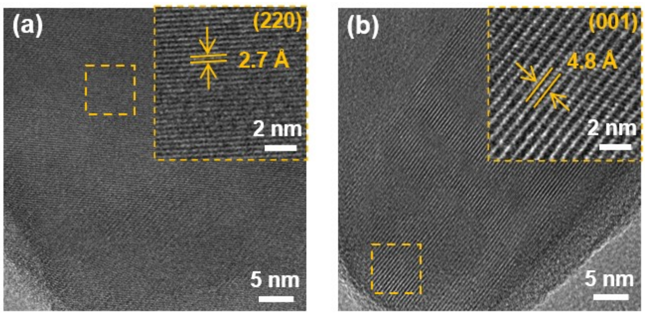

Fig. S5 HRTEM images of (a) κ-$Na_xV_2O_5$ and (b) α'-$Na_xV_2O_5$ phase in MP-NVO-1.

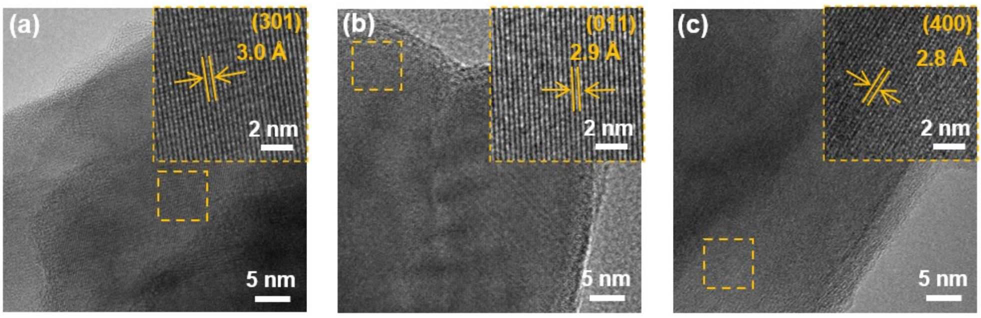

Fig. S6 HRTEM images of SP-NVO.

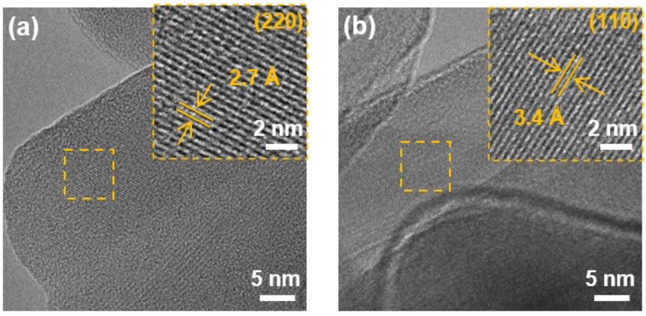

Fig. S7 HRTEM images of (a) κ-$Na_xV_2O_5$ and (b) α'-$Na_xV_2O_5$ phase in MP-NVO-2.

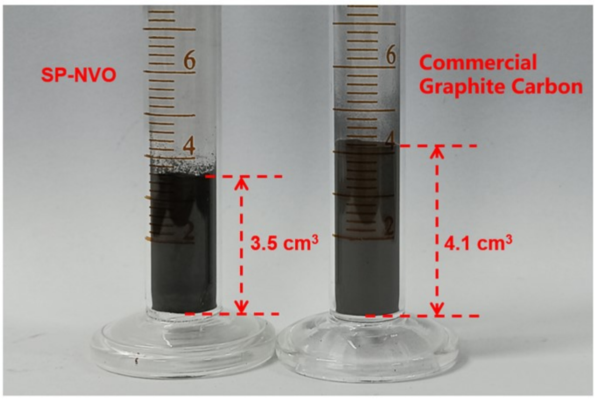

Fig. S8 Comparison of volume between SP-NVO and commercial graphite with same mass.

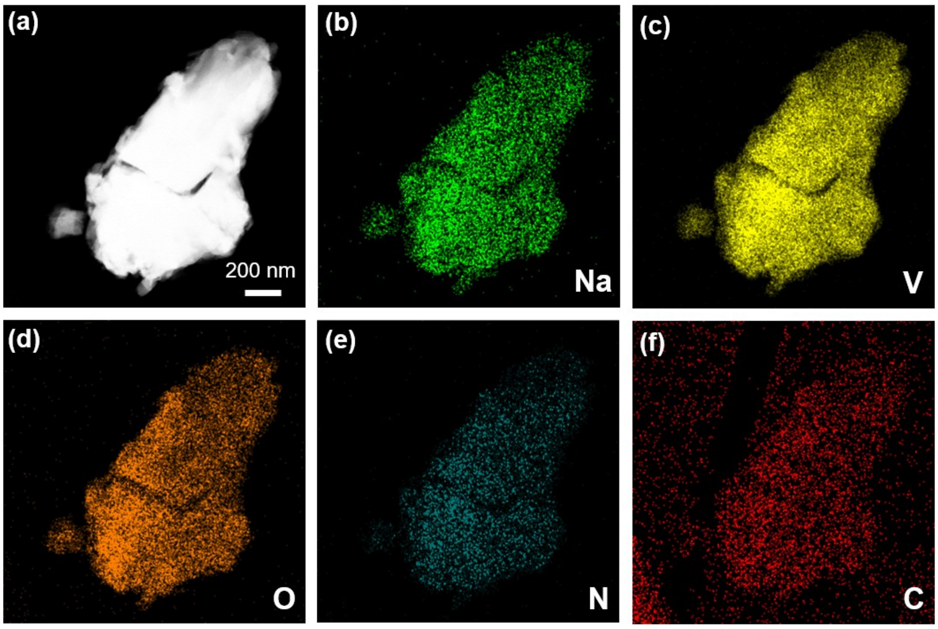

Fig. S9 Elemental mapping images of SP-NVO.

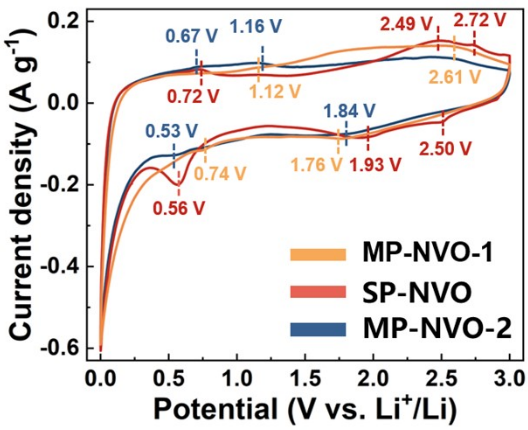

Fig. S10 CV curves of MP-NVO-1, SP-NVO and MP-NVO-2 electrodes at 0.2 mV s^{-1}.

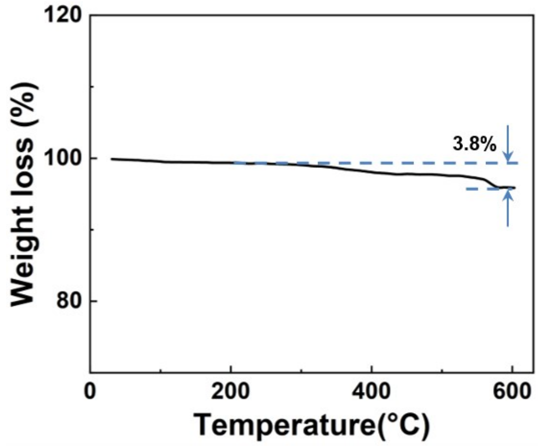

Fig. S11 TG curve of SP-NVO sample.

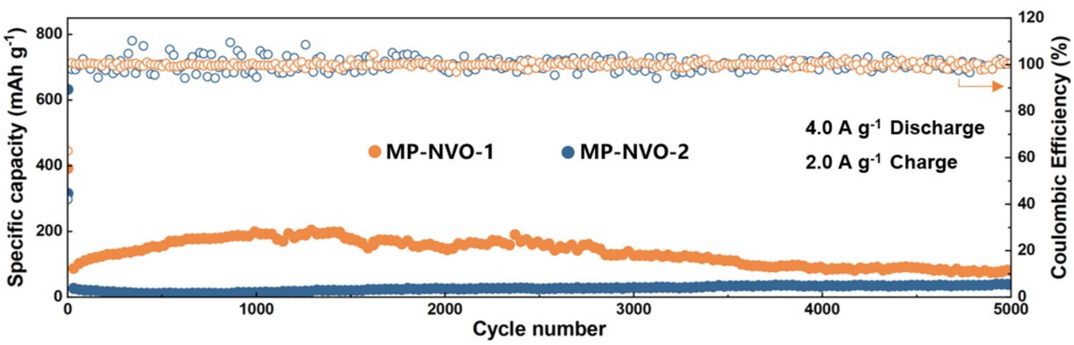

Fig. S12 Cycling performance of MP-NVO-1 and MP-NVO-2 electrodes at a charging/discharging current of 2.0/4.0 A g^{-1}.

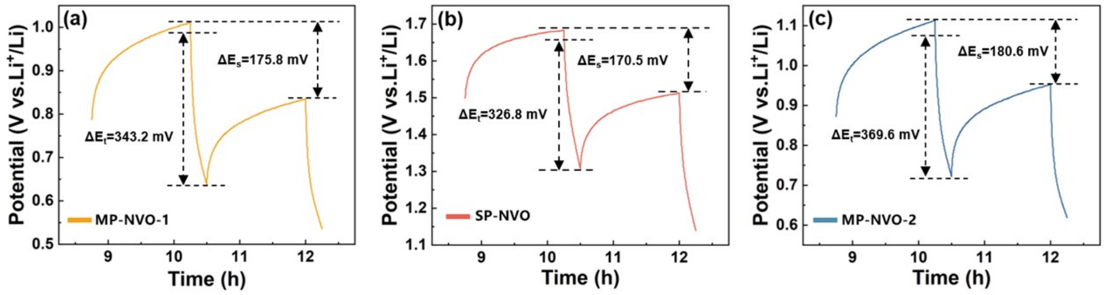

Fig. S13 Single GITT procedure for (a) MP-NVO-1, (b) SP-NVO and (c) MP-NVO-2 electrodes during the discharge process.

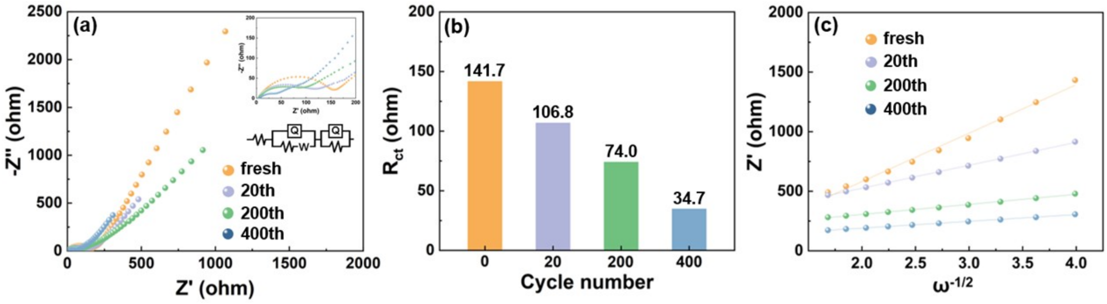

Fig. S14 (a) Nyquist plots, (b) fitted R_{ct} and (c) Z' *vs.*$\omega^{-1/2}$ curves (D_{Li+} determination) of SP-NVO electrode after different cycles.

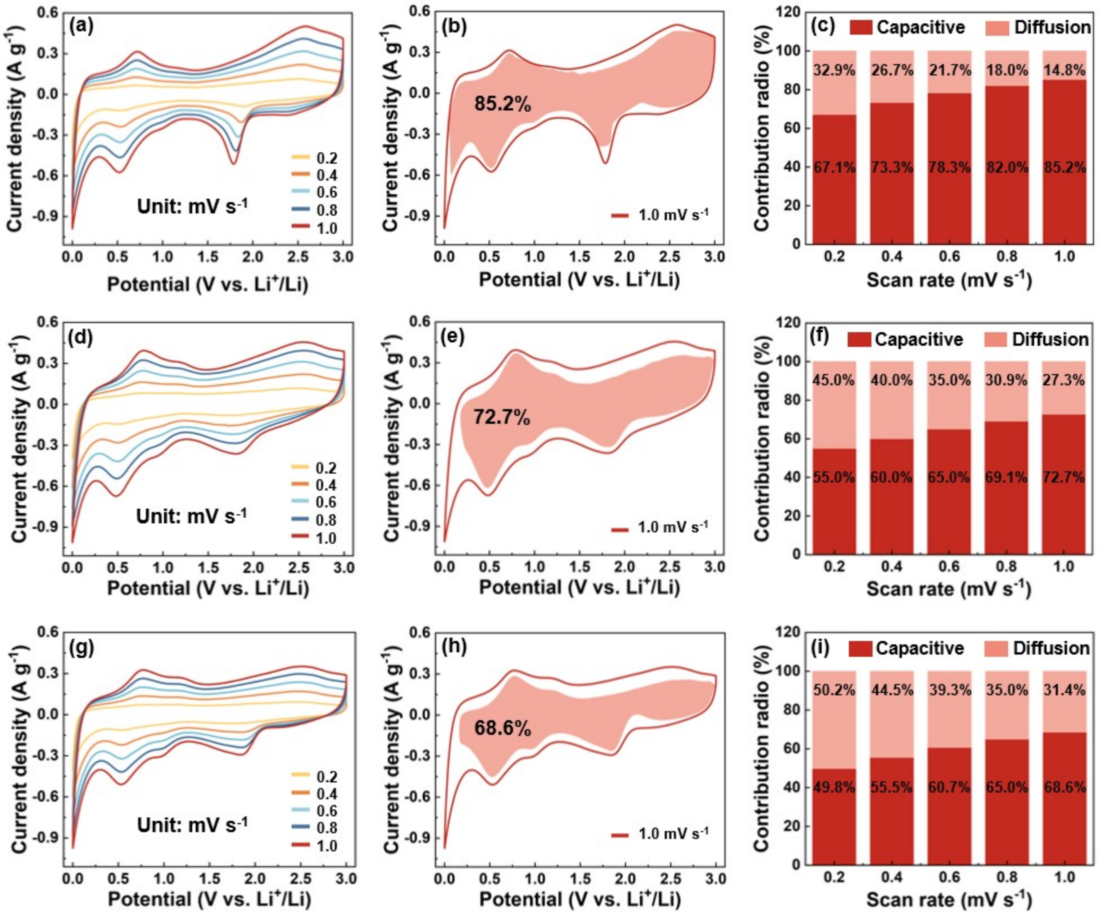

Fig. S15 (a, d, g) CV curves at various scan rates from 0.2 to 1.0 mV s^{-1}, (b, e, h) capacitive energy storage contribution at 1.0 mV s^{-1}, and (c, f, i) capacitive energy storage contribution ratios of (a, b, c) SP-NVO, (d, e, f) MP-NVO-1 and (g, h, i) MP-NVO-2 electrodes.

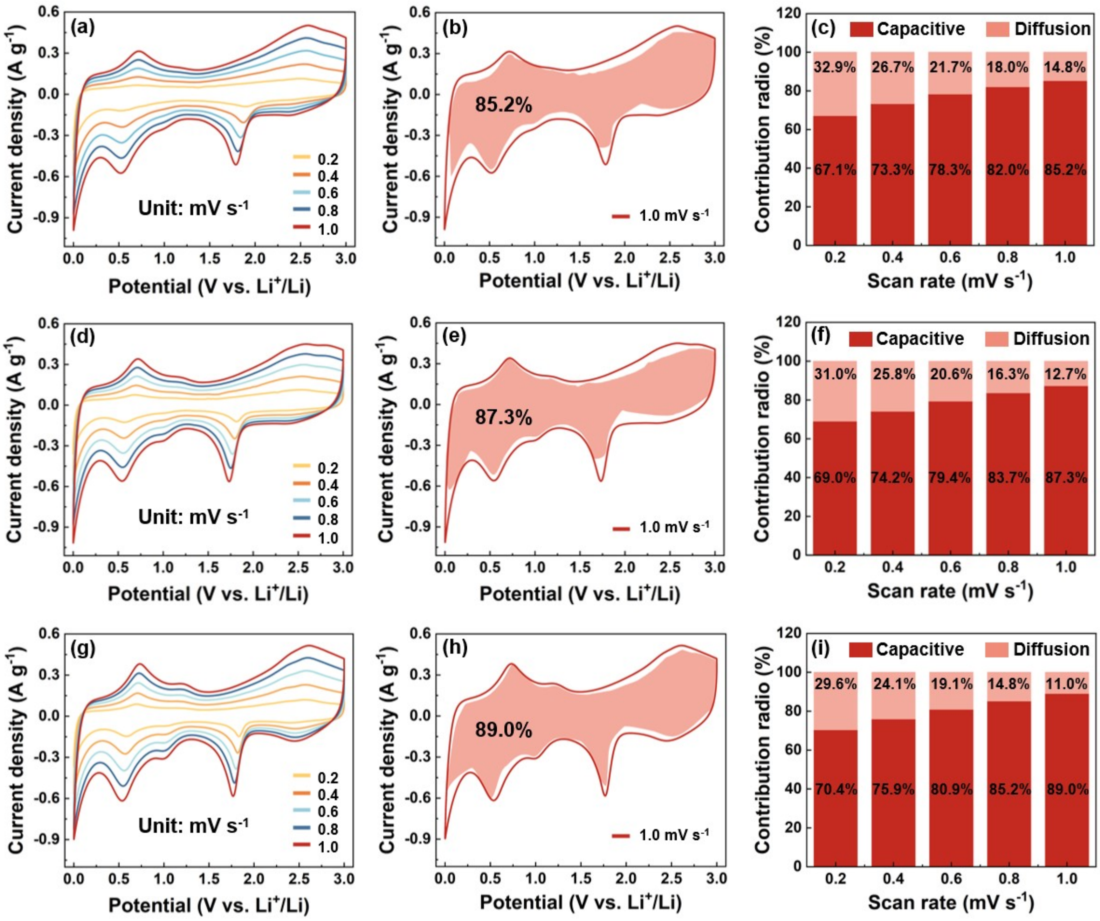

Fig. S16 (a, d, g) CV curves at various scan rates from 0.2 to 1.0 mV s^{-1}, (b, e, h) capacitive energy storage contribution at 1.0 mV s^{-1}, and (c, f, i) capacitive energy storage contribution ratios of SP-NVO (a, b, c) fresh electrode, (d, e, f) cycled electrode after 10 cycles, and (g, h, i) cycled electrode after 20 cycles.

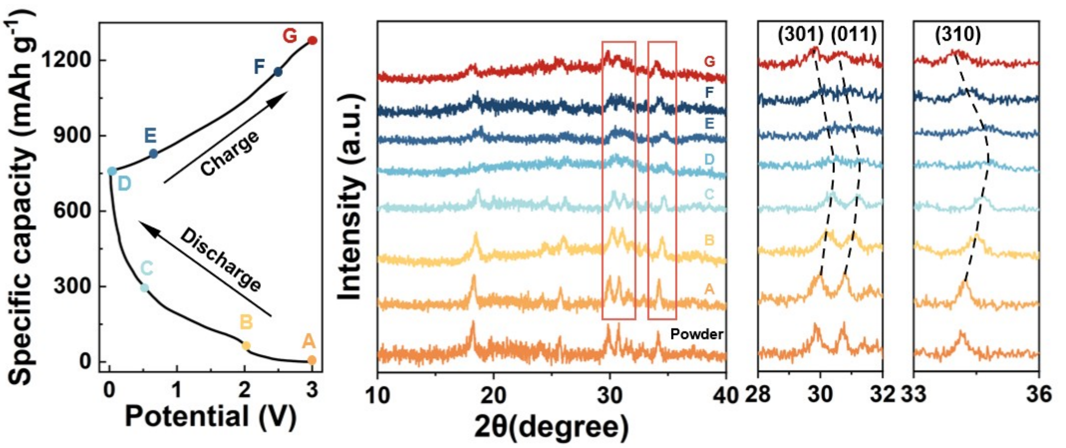

Fig. S17 Ex-situ XRD patterns at different discharge/charge states of SP-NVO electrodes.

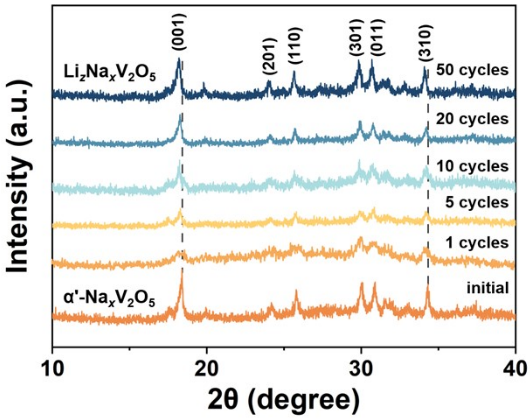

Fig. S18 XRD patterns of cycled SP-NVO electrode after different cycles.

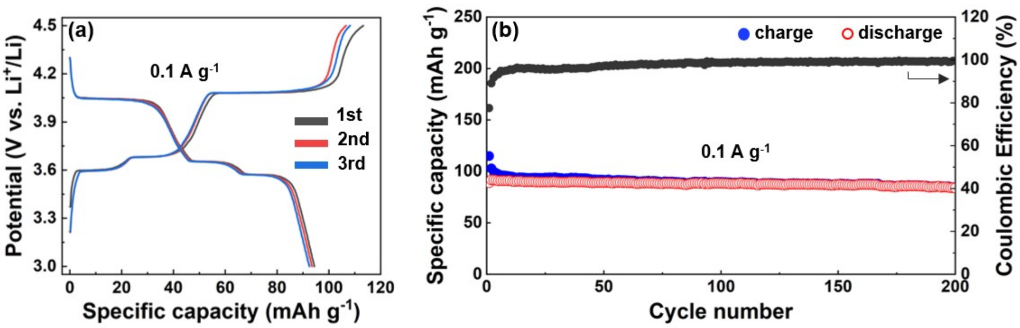

Fig. S19 (a) Galvanostatic charge-discharge profiles and (b) cycling performance of $Li_3V_2(PO_4)_3$ at 0.1 A g^{-1}.

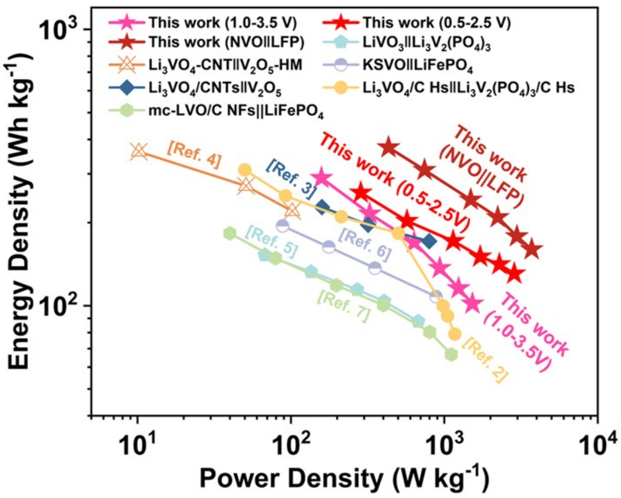

Fig. S20 Ragone plots of SP-NVO‖$Li_3V_2(PO_4)_3$ compared to the previously reported vanadium-based full cells.

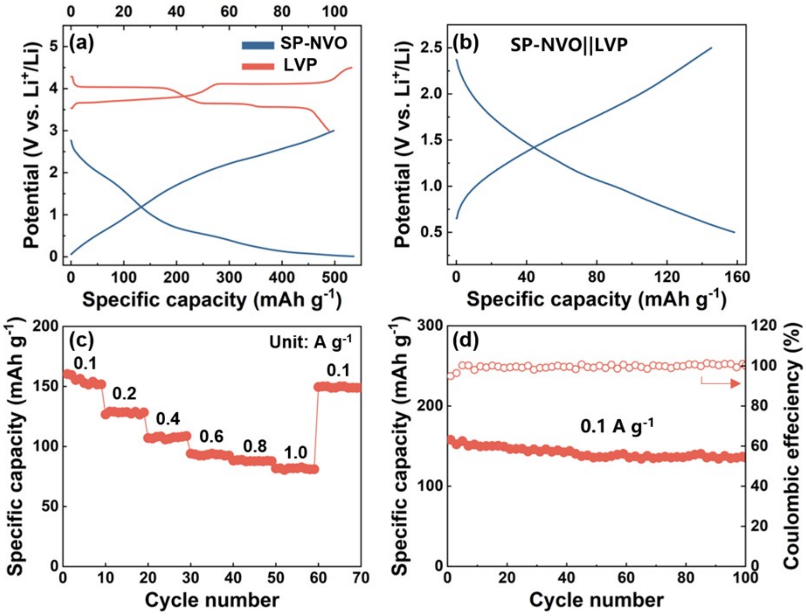

Fig. S21 Electrochemical performance of SP-NVO‖$Li_3V_2(PO_4)_3$ Li-ion full cell at 0.5~2.5V. (a) charge-discharge profiles of SP-NVO and $Li_3V_2(PO_4)_3$; (b) the corresponding charge-discharge profiles of SP-NVO‖$Li_3V_2(PO_4)_3$ full cell; (c) rate performance and (d) cycling performance of SP-NVO‖$Li_3V_2(PO_4)_3$ full cell.

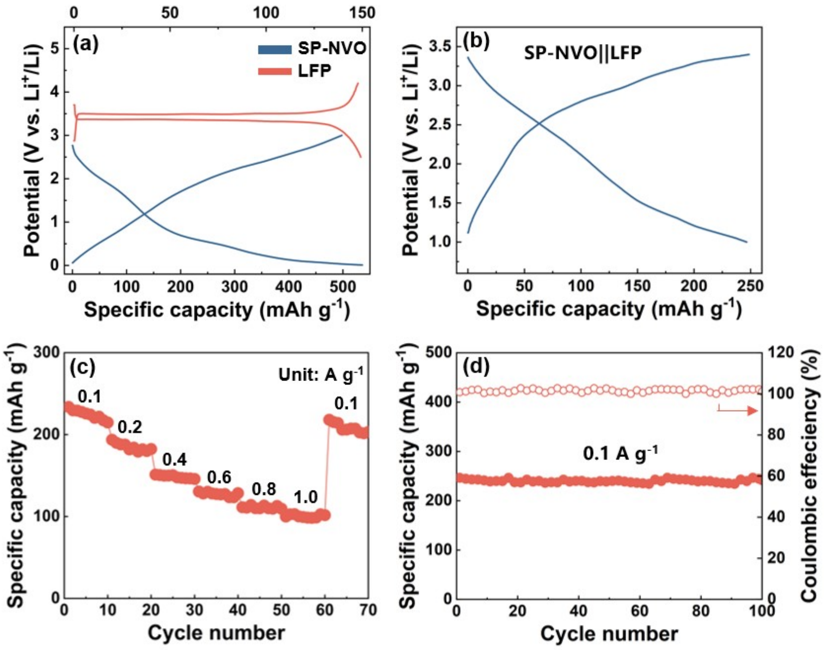

Fig. S22 Electrochemical performance of SP-NVO‖$LiFePO_4$ Li-ion full cell at 1.0~3.5V. (a) charge-discharge profiles of SP-NVO and $LiFePO_4$; (b) the corresponding charge-discharge profiles of SP-NVO‖$LiFePO_4$ full cell; (c) rate performance and (d) cycling performance of SP-NVO‖$LiFePO_4$ full cell.

Table S1 The V^{4+}/V^{5+}molar ratios of $Na_xV_2O_5$ samples.

Samples	The peak area of V^{4+}	The peak area of V^{5+}	The molar ratio V^{4+}/V^{5+} (%)	The reduced content of V^{5+} to V^{4+} (%)	The formula
MP-NVO-1	33487.3 eV	140198.2 eV	24.0	19.0	$Na_{0.38}V_2O_5$
SP-NVO	33959.3 eV	68418.4 eV	49.6	33.3	$Na_{0.67}V_2O_5$
MP-NVO-2	55874.3 eV	56335.4 eV	99.2	49.8	$Na_{1.00}V_2O_5$

The value of x in the as-synthesized $Na_xV_2O_5$ samples is determined based on XPS spectra. For a homogeneous sample containing n elements, the molar concentration of element i can be calculated using the following formula[1]:

$$x_i = \frac{A_i/s_i}{\sum_{j=1}^{n}(A_j/s_j)} \tag{S1}$$

Where A_i is the area under the corresponding core-level peak, and s_i is the relative sensitivity factor (RSF), which is a value determined experimentally under the same instrument and conditions for each core-level peak.

Table S2 The Li^+ diffusion coefficient values of $Na_xV_2O_5$ samples at different discharge/charge states.

Material	State	Potential (V)	D ($cm^2\ s^{-1}$)	State	Potential (V)	D ($cm^2\ s^{-1}$)
SP-NVO	Discharge	2.19	1.77×10^{-12}	Charge	0.34	4.60×10^{-11}
		1.99	3.02×10^{-12}		0.53	1.23×10^{-11}
		1.81	3.22×10^{-12}		0.68	9.20×10^{-12}
		1.59	2.78×10^{-12}		0.82	5.48×10^{-12}
		1.35	1.49×10^{-12}		0.95	3.21×10^{-12}
		1.13	2.63×10^{-12}		1.07	3.03×10^{-12}
		0.98	2.09×10^{-12}		1.19	2.23×10^{-12}
		0.86	1.24×10^{-12}		1.33	1.36×10^{-12}
		0.74	1.23×10^{-12}		1.49	1.07×10^{-12}
		0.64	2.22×10^{-12}		1.64	9.29×10^{-13}
		0.55	2.55×10^{-12}		1.78	9.46×10^{-13}
		0.46	9.91×10^{-13}		1.93	1.02×10^{-12}
		0.30	4.14×10^{-13}		2.07	1.09×10^{-12}
		0.28	2.51×10^{-13}		2.19	1.09×10^{-12}
		0.22	1.62×10^{-13}		2.31	1.22×10^{-12}
		0.17	9.60×10^{-14}		2.42	1.44×10^{-12}
		0.14	4.83×10^{-14}		2.54	1.75×10^{-12}
		0.13	2.13×10^{-11}			
		Average D_{Li+}	**2.64×10^{-12}**		**Average D_{Li+}**	**5.49×10^{-12}**
MP-NVO-1	Discharge	2.14	7.87×10^{-12}	Charge	0.37	4.94×10^{-11}
		1.90	4.45×10^{-12}		0.56	1.24×10^{-11}
		1.64	1.19×10^{-12}		0.72	7.20×10^{-12}
		1.25	7.96×10^{-13}		0.88	3.61×10^{-12}
		0.99	7.52×10^{-13}		1.05	1.97×10^{-12}
		0.82	6.04×10^{-13}		1.24	8.02×10^{-13}
		0.68	1.01×10^{-12}		1.45	4.69×10^{-13}
		0.58	1.29×10^{-12}		1.64	4.02×10^{-13}
		0.47	8.79×10^{-13}		1.79	3.46×10^{-13}
		0.37	3.83×10^{-13}		1.94	3.42×10^{-13}
		0.28	1.76×10^{-13}		2.07	3.80×10^{-13}
		0.22	7.68×10^{-14}		2.18	4.57×10^{-13}
		0.20	2.02×10^{-14}		2.29	6.36×10^{-13}
		0.18	1.74×10^{-15}		2.41	9.88×10^{-13}
		0.17	3.49×10^{-15}		2.53	1.23×10^{-12}
		0.15	5.52×10^{-15}		2.65	1.63×10^{-12}
		0.14	1.55×10^{-11}			
		Average D_{Li+}	**2.06×10^{-12}**		**Average D_{Li+}**	**5.14×10^{-12}**
MP-NVO-2	Discharge	2.07	5.48×10^{-12}	Charge	0.15	1.36×10^{-11}
		1.87	2.63×10^{-12}		0.35	4.96×10^{-11}
		1.65	1.19×10^{-12}		0.51	8.76×10^{-12}
		1.35	5.32×10^{-13}		0.65	5.47×10^{-12}
		1.08	5.96×10^{-13}		0.78	2.83×10^{-12}
		0.92	4.93×10^{-13}		0.91	1.71×10^{-12}
		0.80	3.87×10^{-13}		1.03	1.06×10^{-12}
		0.70	4.69×10^{-13}		1.16	5.26×10^{-13}
		0.60	8.25×10^{-13}		1.33	3.28×10^{-13}
		0.52	7.84×10^{-13}		1.48	2.16×10^{-13}
		0.44	3.80×10^{-13}		1.63	1.66×10^{-13}
		0.37	1.59×10^{-13}		1.76	1.73×10^{-13}
		0.31	1.10×10^{-13}		1.87	1.81×10^{-13}
		0.25	7.01×10^{-14}		1.98	1.65×10^{-13}
		0.22	2.09×10^{-14}		2.08	1.84×10^{-13}
		0.20	5.87×10^{-15}		2.17	2.23×10^{-13}
		0.19	3.18×10^{-15}		2.27	3.21×10^{-13}
		0.18	1.29×10^{-15}		2.37	3.87×10^{-13}
		0.17	1.30×10^{-15}		2.47	4.63×10^{-13}
		0.16	6.00×10^{-15}		2.58	4.96×10^{-13}
		0.14	1.57×10^{-15}			
		Average D_{Li+}	**6.73×10^{-13}**		**Average D_{Li+}**	**4.13×10^{-12}**

Table S3 The summarization of cycling performance of vanadium-based full cells.

Material	Energy density (Wh kg^{-1})	Power density (W kg^{-1})	Discharge current (mA g^{-1})	Capacity (mAh g^{-1})	Capacity retention	Ref.
Li_3VO_4/C Hs‖$Li_3V_2(PO_4)_3$/C Hs	50.0	310.0	1000	274.0	56.4%	[2]
Li_3VO_4/CNTs‖V_2O_5	159.2	227.5	1000	62.0	71.4%	[3]
Li_3VO_4-CNT‖V_2O_5-HM	10.0	284.0	0.67C	100.0	71.3%	[4]
$LiVO_3$‖$Li_3V_2(PO_4)_3$	67.5	152.7	50	112.0	70.4%	[5]
KSVO‖$LiFePO_4$	194.4	88.2	1000	36.0	95.1%	[6]
mc-LVO/C NFs‖$LiFePO_4$	40.0	182.8	500	282.0	86.1%	[7]
α'-$Na_xV_2O_5$‖$Li_3V_2(PO_4)_3$ (0.5-2.5 V)	**285.7**	**256.0**	**100**	**135.7**	**87.0%**	**This work**
α'-$Na_xV_2O_5$‖$Li_3V_2(PO_4)_3$ (1-3.5 V)	**158.1**	**289.9**	**100**	**144.8**	**86.6%**	
α'-$Na_xV_2O_5$‖$LiFePO_4$	**374.1**	**432.9**	**100**	**241.9**	**98.0%**	

References

1. G. Greczynski and L. Hultman, *Prog. Mater. Sci.*, 2020, **107**, 100591.

2. X. Bai, D. Li, D. Zhang, S. Yang, C. Pei, B. Sun and S. Ni, *J. Mater. Chem. A*, 2023, **11**, 12164−12175.

3. Y. Shan, L. Xu, Y. Hu, H. Jiang and C. Li, *Chem. Eng. Sci.*, 2019, **200**, 38−45.

4. P. Zhang, L. Zhao, Q. An, Q. Wei, L. Zhou, X. Wei, J. Sheng and L. Mai, *Small*, 2016, **12**, 1082−1090.

5. S. Shao, B. Liu, M. Zhang, J. Yin, Y. Gao, K. Ye, J. Yan, G. Wang, K. Zhu and D. Cao, *J. Energy Storage*, 2021, **35**, 102254.

6. Q. Zhang, S. Ma, W. Wang, S. Gao, Y. Ou, S. Li, X. Liu and C. Lin, *Energy Storage Mater.*, 2022, **52**, 637−645.

7. L. Kuang, B. Sun, S. Yang, D. Zhang, C. Pei, P. Li, T. Xiao and S. Ni, *J. Mater. Chem. A*, 2024, **12**, 4008−4018.